Creep, Shrinkage and Durability Mechanics of Concrete and other Quasi-Brittle Materials
Edited by F.-J. Ulm, Z.P. Bažant and F.H. Wittmann

3D Lattice Model for Dynamic Simulations of Creep, Fracturing and Rate Effect in Concrete

Gianluca Cusatis [a] *, Zdeněk P. Bažant[b] and Luigi Cedolin [a] *

[a]Department of Structural Engineering, Politecnico di Milano
P.za Leonardo da Vinci, 32 - 20133 Milano, Italy

[b]Department of Civil Engineering, Northwestern University
2145 Sheridan Road, Evanston, Illinois 60208-3109, USA

As verified experimentally, the rate dependence of the deformations of concrete is caused by two different physical mechanisms. The first is a dependence of the fracture process on the rate of crack opening, and the second is the viscoelastic deformation of cement paste. In this paper, the first is described by the activation energy theory applied to the ruptures that occur along a cohesive crack, and the second by the microprestress-solidification theory of concrete creep. Both theories are implemented in a recently developed three-dimensional lattice model that is able to simulate the static nonlinear uniaxial and triaxial behavior of concrete. Some numerical simulations are carried out to validate the model.

1. INTRODUCTION

The behavior of concrete under various types of loading is strongly affected by the heterogeneous character of its internal structure. This heterogeneity leads to a non-uniform stress distribution at the meso-level even if at the macroscopic level the stresses are uniform. Since failure of concrete usually evolves as progressive internal damage, it is useful directly simulate with the mathematical model the processes under way at the meso-level during failure. This can be accomplished with the lattice models. In this work, a lattice model recently developed fo the time independent behavior [6], [7] is used. After presenting it, the model will be extended to time-dependent behavior with emphasis on creep and rate dependence of fracture.

2. REVIEW OF THE MODEL

The geometrical structure of the model can emulate the mix design of concrete. Given the aggregate-cement ratio, a/c, the cement content, c and the sieve curve, we can calculate for a given specimen of volume V the number n_i of aggregates with characteristic dimension that lies in specified interval of average dimension D_i; $n_i = \psi_i M_a/\rho_a v_i$ where $v_i = \pi D_i^3/6$ is the volume of an aggregate, ψ_i is the ratio between the mass of aggregates which have characteristic dimension D_i and the total mass of aggregates, $M_a = (a/c)cV$,

*Financial support of European Commission (ANCHR Project) is gratefully acknowledged.

and ρ_a is the mass density of aggregates. The mathematical generation of the lattice simulates random placing of the aggregates, one-by-one, into a form in which the concrete specimen is cast. The placements begin the aggregates with the largest size and proceeds until the last aggregate of the smallest size has been placed. The geometrical arrangement of the aggregates is based on a lattice constructed through the Delaunay triangulation. Each ridge of each Delaunay tetrahedron represents a connecting strut between two aggregates. Within each connecting strut, a point at which the forces between the aggregates are imagined to be transmitted is defined. With reference to Fig. 1a, we assume $L_1 = LD_1/(D_1 + D_2)$, $L_2 = LD_2/(D_1 + D_2)$.

The kinematics of the model is defined assuming that: 1) the axial velocity $\dot{u}$ is linearly distributed between the aggregate centers (lattice nodes), and 2) the transversal velocities $\dot{v}$, $\dot{w}$ are the effect of a rigid motion corresponding to the motion at point 1, for side 13, and at point 2 for side 24 (see Fig. 1b). The transversal velocities at the interaction point can be then computed as $\dot{v}_3 = \dot{v}_1 + L_1\dot{\vartheta}_1$, $\dot{v}_4 = \dot{v}_2 - L_2\dot{\vartheta}_2$, $\dot{w}_3 = \dot{w}_1 - L_1\dot{\varphi}_1$ and $\dot{w}_4 = \dot{w}_2 + L_2\dot{\varphi}_2$.

The assumed measures of strain are related to the relative displacements in the axial direction N and to the transversal relative displacements in two orthogonal directions M and L at the interaction point. We can write $\dot{\varepsilon}_N = (\dot{u}_2 - \dot{u}_1)/L$, $\dot{\varepsilon}_M = (\dot{v}_4 - \dot{v}_3)/L = (\dot{v}_2 - \dot{v}_1 - L_2\dot{\vartheta}_2 - L_1\dot{\vartheta}_1)/L$ and $\dot{\varepsilon}_L = (\dot{w}_4 - \dot{w}_3)/L = (\dot{w}_2 - \dot{w}_1 + L_2\dot{\varphi}_2 + L_1\dot{\varphi}_1)/L$.

The constitutive relation is characterized by the behavior of the interface at the contact point. The initial elastic behavior can be expressed as $\sigma_N = E_{N0}\,\varepsilon_N$, $\sigma_M = E_{T0}\,\varepsilon_M$ and $\sigma_L = E_{T0}\,\varepsilon_L$. The previous elastic relations are equivalent to $\sigma = E_0\,\varepsilon$;

$$\sigma_N = \sigma\varepsilon_N/\varepsilon \quad \sigma_M = \sigma\alpha\varepsilon_M/\varepsilon \quad \sigma_L = \sigma\alpha\varepsilon_L/\varepsilon \tag{1}$$

where $E_0 = E_{N0}$, $\alpha = E_{T0}/E_{N0}$, $\varepsilon = \sqrt{\varepsilon_N^2 + \alpha^2\varepsilon_T^2}$ and $\varepsilon_T = \sqrt{\varepsilon_M^2 + \varepsilon_L^2}$

The elastic modulus E_0 must be computed preserving the different elastic properties of cement and aggregates. Assuming a series coupling, we have

$$E_0 = E_c L/(rL_a + L_c) \tag{2}$$

where E_c is the elastic modulus of the cement paste, $r = E_c/E_a$ is ratio between the elastic moduli of cement paste and aggregates, $L_a = (D_1 + D_2)/2$ and $L_c = L - L_a$.

The stress-strain evolution remains elastic as far as σ does not reach a certain strength limit. Afterwards the evolution follows a given stress-strain boundary (analogous to the boundary used in microplane model [2]). If unloading occurs, the behavior is considered to be hypo-elastic. The following equations govern the inelastic regime:

$$\dot{\sigma} = E(\varepsilon,\omega)\,\dot{\varepsilon} \quad 0 \le \sigma \le \sigma_b(\varepsilon,\omega) \tag{3}$$

where ω, defined by $\tan\omega = \varepsilon_N/(\alpha\varepsilon_T)$, represents a generalized strain measure that characterizes the coupling between the normal and shear stresses (pure shear for $\omega = 0$, pure tension for $\omega = \pi/2$, pure compression for $\omega = -\pi/2$, shear-tension coupling for $0 < \omega < \pi/2$, and shear-compression coupling for $-\pi/2 < \omega < 0$). The tangent elastic modulus is assumed equal to E_0 for $\omega < 0$ (as in plasticity theory), equal to the secant modulus σ/ε for $\omega = \pi/2$ (as in damage theory) and equal to a linear interpolation between these two limit cases for $0 < \omega < \pi/2$. From Eq. 3, one can calculate the normal and shear stresses assuming that Eqs. 1 remain valid during elastic as well inelastic behavior.

The stress-strain boundary is defined by the equation

$$\sigma_b(\varepsilon,\omega) = \sigma_0(\omega)\exp\left\{\frac{K(\omega)\,\langle\varepsilon - \varepsilon_0(\omega)\rangle}{\sigma_0(\omega)}\right\} \tag{4}$$

where $\varepsilon_0(\omega) = \sigma_0(\omega)/E_0$. The function $\sigma_0(\omega)$ is the strength limit and, because of Eq. 1, it can be represented in the stress space (σ_N, σ_T) as the usual elastic domain. In this work, the assumed elastic domain is a hyperbola with a cut-off in compression (Fig. 1c). The analytical expression of $\sigma_0(\omega)$ depends on tensile strength σ_t, shear strength (cohesion) σ_s, compressive strength σ_c and friction μ. $K(\omega)$ is the slope of the boundary $\sigma_b(\omega)$ for $\varepsilon = \varepsilon_0(\omega)$. In the case of pure tension, a softening behavior is assumed, $K(\pi/2) = -K_t < 0$, while in the case of pure compression, hardening behavior is assumed, $K(-\pi/2) = K_c > 0$. The transition between softening and hardening is made assuming perfect plastic behavior in the case of pure shear, $K(0) = 0$. For intermediate values of ω, the expression for $K(\omega)$ is obtained by linear interpolation. The softening modulus K_t is not a material parameter because it depends on the length of the element L in order to preserve the correct energy dissipation during crack propagation, $K_t = 2E_0/(L_{cr}/L - 1)$ where $L_{cr} = 2E_0G_f/\sigma_t^2$. The details of the formulation appear in [6].

3. INCORPORATION OF CREEP

One of sources of the rate effect in concrete is the viscoelastic nature of the cement paste which is modeled in this paper through the microprestress-solidification theory [3]. The equation $\dot{\sigma} = E\dot{\varepsilon}$ should then be replaced by the differential equations which describe the evolution of an aging Maxwell chain or, equivalently, by the integral equation obtained through the compliance function $J(t,t')$ following from the theory. However, since only dynamic applications will be considered, it suffices to use just one term of the Maxwell chain, represented by the differential equation

$$\dot{\sigma} + \sigma/\tau = E\dot{\varepsilon} \tag{5}$$

where $\tau = \eta/E$ is the relaxation time. E is equal to E_0 as long as no damage occurs, and afterwards the same loading-unloading rule as in the preceding section is followed. The initial elastic modulus E_0 and the viscosity η must, once again, be computed taking into account the different properties of aggregate and cement paste. Assuming a series coupling between these two constituents, we get again Eq. 2 and $\eta = \eta_c L/L_c$. The viscoelastic properties of cement paste E_c, η_c can be obtained following [5], in which the Maxwell model is identified by requiring its compliance function to be tangent to the actual compliance function $J(t,t')$ at the time $t_{ch} = t_{load}/2$ where t_{load} is the duration of the dynamic event. From this condition one obtains $E_c = 1/(J_{ch} - t_{ch}\dot{J}_{ch})$ and $\eta_c = 1/\dot{J}_{ch}$ where $J_{ch} = J(t' + t_{ch}, t')$, $\dot{J}_{ch} = \dot{J}(t' + t_{ch}, t')$, t'= age at loading.

4. RATE DEPENDENCE OF STRESS-STRAIN BOUNDARY

To take into account only the rate effect in concrete creep (material viscoelasticity) would be insufficient. Recently it has been shown that concrete exhibits a reversal of soft-

ening into hardening after a sudden increase of the loading rate [4], [9]. This phenomenon cannot be modeled by material viscoelasticity. Rather, it can be modeled only trough a rate dependence of the fracture processes. By using activation energy theory, Bažant [1] showed that in concrete the rate dependence of crack opening can be expressed, at reference temperature ($T = T_0 \approx 23°C$), as $\dot{w} = k_0 \sinh[k_r^{-1} N_b(w)^{-1}(\sigma - f^0(w))]$ where k_0 and k_r are constants, $f^0(w)$ is the cohesive law observed for the rate of loading typical of the static material tests in the laboratory, and $N_b(w)$ is the number of bonds across the cohesive crack that still have load-carrying capacity. Assuming $N_b(w) \propto f^0(w)$ and solving the previous equation for σ, we get

$$\sigma(w, \dot{w}) = [1 + k_1 \operatorname{asinh}(\dot{w}/k_0)] f^0(w) \tag{6}$$

which represents a vertical scaling of the static cohesive law by a function of the crack opening rate.

In the present model, the rate dependence can then be introduced, adhering to similarity with Eq. 6, by scaling the stress-strain boundary 4 by a function of the strain rate $\dot{\varepsilon}$

$$\sigma_b(\varepsilon, \dot{\varepsilon}, \omega) = F(\dot{\varepsilon})\, \sigma_0(\omega) \exp\left\{ \frac{K(\omega)\,\langle \varepsilon - \varepsilon_0(\omega) \rangle}{\sigma_0(\omega)} \right\} \tag{7}$$

where $F(\dot{\varepsilon}) = [1 + c_1 \operatorname{asinh}(\dot{\varepsilon}/c_0)]$.

5. VALIDATION BY FITTING OF TEST DATA

The preceding formulation has been implemented in a finite element code for dynamic analysis based on an explicit integration scheme. The code as been used to validate the model by simulating uniaxial tensile and compressive tests at various strain rates.

A prismatic specimen has been considered using the following material properties: $a/c = 5.5$, $c = 320$ Kg/m^3, $\rho_a = 2880$ Kg/m^3. The assumed granulometric distribution is described in Table 1. Fig. 1d shows the resulting lattice in which 2815 finite elements connect 404 aggregates generated by the random procedure. The results of the numerical simulations in the case of compression are compared with experimental tests by Dilger [8] in Fig. 1e. These data are relevant to three different strain rates 3.3×10^{-5}, 3.3×10^{-3} and 2.0×10^{-1} sec^{-1}. The fits have been obtained by setting the parameters of the model as follows: $\alpha = 0.25$, $r = 6$, $\sigma_t = 6$ MPa, $G_f = 0.04$ N/mm, $\sigma_c = 13\sigma_t$, $K_c = 0.01\, E_c$, $\sigma_s = 3\sigma_t$, $\mu = 0.6$, $a_V = 0.5$, $c_0 = 1 \times 10^{-6}$ sec^{-1} and $c_1 = 5 \times 10^{-2}$. The elastic modulus E_c and the viscosity η_c are computed from the compliance function $J(t, t')$ of the microprestress-solidification theory for basic creep. The compliance function depends on four parameters q_1,..., q_4 which have been optimized in order to get the initial slope of Dilger's experimental data, $q_1 = 1.7 \times 10^{-5}$ MPa^{-1}, $q_2 = 3.2 \times 10^{-5}$ MPa^{-1}, $q_3 = 0.9 \times 10^{-6}$ MPa^{-1} and $q_4 = 3.5 \times 10^{-6}$ MPa^{-1}. The procedure for computing E_c and η_c also requires the values of the age of concrete t' and the duration of loading t_{load}. The age was assumed as $t' = 28$ day, and the duration of loading was considered as 180, 1.8 and 0.03 s, respectively, for the three different strain rates. With these model parameters, the tensile tests have been simulated for the same strain rates as in compression. The results (Fig. 1) confirm that the peak obtained for tension is about 1/10 of the peak for compression, as it should.

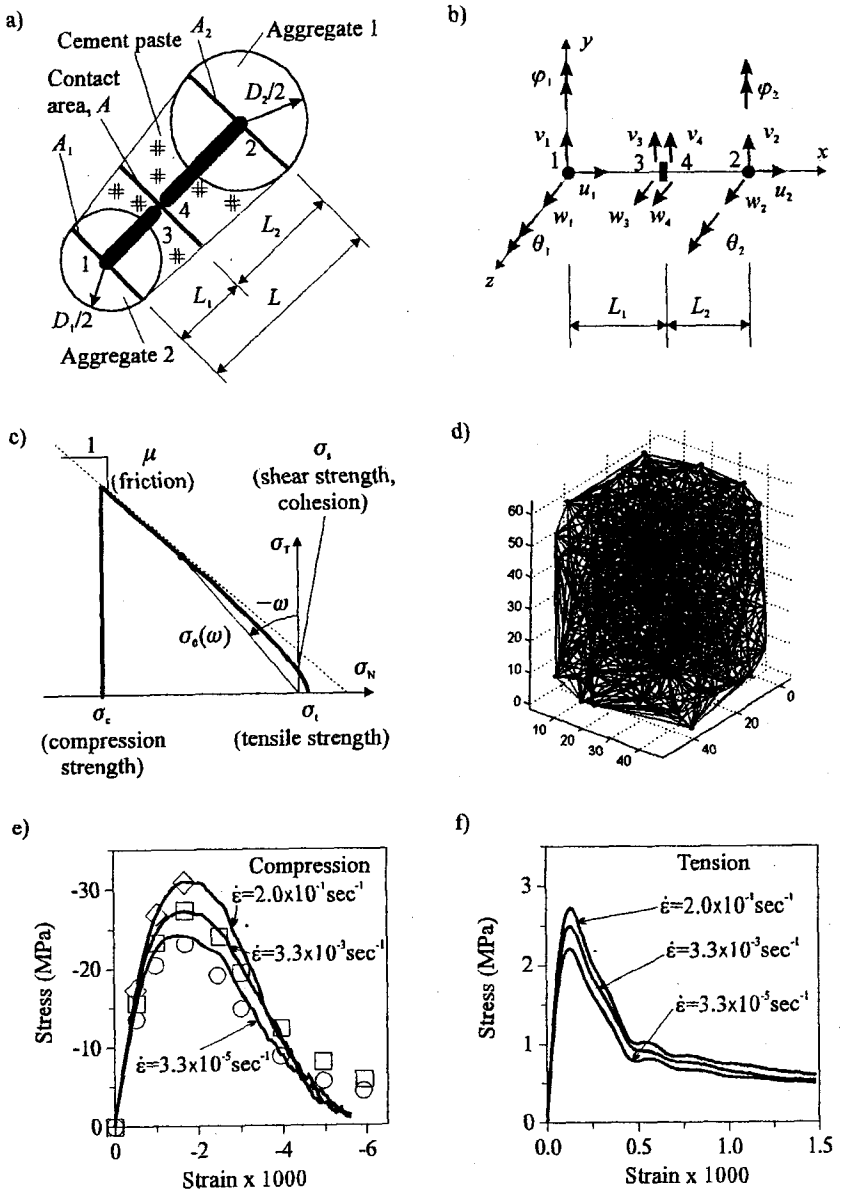

Figure 1. a) Particle definition; b) Kinematic conventions; c) Elastic domain; d) Generated lattice; e), f) Results for compression and tension.

Table 1
Granulometric distribution used in calculations

	size 1	size 2	size 3	size 4	size 5	size 6
Diameter, D_i in mm	16	10	8	7	5	4
Amount, % in mass	12	12	7	7	6	7

6. CONCLUSIONS

1. The new lattice model, previously developed for static applications, has been generalized by introducing in the time-dependence of the deformations of concrete.

2. The rate effect in concrete response has been analyzed and numerical simulations have shown a good agreement with the experimental data from the literature. Validation and calibration by more extensive test results is nevertheless desirable.

3. The present model can also simulate long-term creep and shrinkage of fracturing concrete if the full microprestress-solidification theory is used instead of the present replacement of the Maxwell chain by a single Kelvin unit.

REFERENCES

1. Bažant Z.P., Creep and damage in concrete. Materials science of concrete IV, (1995) 355-389.
2. Bažant Z.P., Caner F., Carol I., Adley M. and Akers S. Microplane Model M4 for concrete. I: Formulation with Work-Conjugate Deviatoric Stress. J. of Engrg. Mech., ASCE, 1236 (2000) 944-953.
3. Bažant Z.P., Hauggaard A.B., Baweja S. and Ulm F.J., Microprestress-Solidification Theory for Concrete Creep. I: Aging and Drying Effects. J. of Engrg. Mech., ASCE, 123 (1997) 1188-1194.
4. Bažant Z.P., Gu W.H. and Faber K.T., Softening reversal and other effects of a change in loading rate on fracture. ACI Mat. J., 92 (1995) 3-9.
5. Bažant Z.P., Caner F.C., Adley M.D. and Akers S.A., Fracturing rate effect and creep in microplane model for dynamics. J. of Engrg. Mech., ASCE, 126 (2000) 962-970.
6. Cusatis G., Bažant Z.P. and Cedolin L., 3D random lattice model for concrete. I: Formulation, submitted for pubblication
7. Cusatis G., Bažant Z.P. and Cedolin L., 3D random lattice model for concrete. II: Numerical implementation and calibration, submitted for pubblication
8. Dilger W.H., Koch R. and Kowalczyk R., Ductility of plain and confined concrete under different strain rates, Am. Concrete Inst. Spec. Publ., Detroit, Mich.
9. Tandon S., Faber K., Bažant Z.P. and Li Y.N., Cohesive crack modeling of influence of sudden changes in loading rate on concrete fracture. Engrg. Fracture Mech. 52 (1995) 987-997.